JOURNAL OF AIRCRAFT
Vol. 37, No. 1, January–February 2000

Improvement of a Numerical Procedure for the Dynamic Analysis of Aircraft Structures

Silvano Tizzi*
University of Rome "La Sapienza," 00184 Rome, Italy

A new model (n.m.) of a numerical procedure, which lies between Rayleigh–Ritz and the finite element method (FEM), previously applied for three-dimensional aircraft structures, has been developed to improve the accuracy of the natural frequency values obtained by the old model (o.m.) of this proposed method (PM). The basic characteristic of this n.m. consists in utilizing local describing functions defined in each single-plate component element together with the global describing ones, defined in all of the space containing the structure, already employed in the o.m. of PM. First, an application of both models to the same tail structure of previous work has been performed for a preliminary comparison between their results. Two further applications of both models to wing and tail structures have been performed. These analyses used a sequence of flat trapezoidal thin plates in a three-dimensional space, connected only in a serial form along the cantilever's length. The analyses were performed with a higher number of component elements than in previous work. A comparison between the results of the two models has been repeated to show the higher accuracy of the vibration frequency values obtained thanks to this n.m., which become more evident as the complexity of the structure grows. The advantages of this n.m. of the PM, particularly with respect to the CPU time, have been pointed out comparing the obtained results also with the ones of a classical FEM numerical program, such as MSC/NASTRAN.

Nomenclature

A = in-plane rigidity modulus
E = elasticity modulus
E_{12} = parameter containing the elasticity modulus
e_{et}, e_{ue}, e_{uevt} = occurring integrals obtained by the local describing functions
G = shear rigidity modulus
$g^{(n)}_{i_a i_b i_c}, g^{(r)}_{i_a i_b i_c}, g^{(s)}_{j_a j_b j_c}$ = global describing functions coefficients of the generic variable S_n
h = nondimensional plate thickness
h' = plate thickness
K = stiffness matrix
L = cantilever's length of the generic plate
L_0 = reference length
$\bar{L}$ = nondimensional cantilever's length of the generic plate
$l^{(I_p)}_{n_{iea,ieb}}, l^{(I_p)}_{r_{iea,ieb}}, l^{(I_p)}_{s_{jea,jeb}}$ = local describing functions coefficients of the generic variable S_n in the I_pth panel
M = mass matrix
N = number of Lagrangian degrees of freedom
N_a, N_b, N_c = number of global describing functions along the axes X, Y, Z, respectively
N_{ea}, N_{eb} = number of local describing functions along X_l and Y_l, respectively
$P_{et}, P_{ue}, P_{ev}, P_{uevt}$ = occurring mixed integrals obtained by the coupling between global and local describing functions
P_{Pt}, P_{uP}, P_{uvt} = occurring integrals obtained by the global describing functions
q_i = generic Lagrangian degree of freedom
R_{ij} = rotation matrix element connecting the axis X_i with the axis X_{lj}
S_n, S_r, S_s = generic independent variable
$U, V, W; U_1, U_2, U_3$ = nondimensional displacements along the axes of the main reference system
$U_l, V_l, W_l; U_{l1}, U_{l2}, U_{l3}$ = nondimensional displacements along the axes of the local reference system
$u, v, w; u_1, u_2, u_3$ = displacements along the axes of the main reference system
$u_l, v_l, w_l; u_{l1}, u_{l2}, u_{l3}$ = displacements along the axes of the local reference system
$X, Y, Z; X_1, X_2, X_3$ = nondimensional coordinates of the main reference system
$X_l, Y_l, Z_l; X_{l1}, X_{l2}, X_{l3}$ = nondimensional coordinates of the local reference system
$x, y, z; x_1, x_2, x_3$ = main reference system
$x_l, y_l, z_l; x_{l1}, x_{l2}, x_{l3}$ = local reference system
δ_b = discriminating parameter
δ_{ij} = Kronecker's delta
$\theta_Y, -\theta_X, \theta_Z; \theta_1; \theta_{l2}.\theta_{l3}$ = rotations along the coordinates of the local reference system
$\theta_x, \theta_y; \theta_z; \theta_1, \theta_2, \theta_3$ = rotations along the coordinates of the main reference system
ρ = mass density
ω = angular frequency
ω_d = nondimensional frequency parameter

Subscripts

$i_a, i_b, i_c; j_a, j_b, j_c$ = symbols referring to the coefficients of the global describing functions
$i_r, j_s; i_{er}, j_{es}$ = symbols referring to the Lagrangian degrees of freedom corresponding to the global and local describing functions, respectively
n, r, s = symbols referring to the generic independent variable
$n_{iea,ieb}, r_{iea,ieb}, s_{jea,jeb}$ = symbols referring to the coefficients of the local describing functions
X, Y, Z = symbols referring to the rotations around the axes of the local reference system
x, y, z = symbols referring to the rotations around the axes of the main reference system

Received 20 December 1998; revision received 17 May 1999; accepted for publication 20 May 1999.

*Researcher, Aerospace Department.

Superscripts

(I_p) = symbol referring to the identification number of the I_pth panel

$(n), (r), (s)$ = symbol referring to the generic independent variable

Introduction

TO increase the accuracy of the obtained results, an improvement of the numerical model of a procedure[1–4] utilized for the dynamic analysis of three-dimensional aircraft structures has been performed. This improved procedure arises from the Rayleigh–Ritz method,[5,6] and it is obtained combining the Ritz analysis with the variational principles,[7–9] like the finite element method (FEM).[10–13] This further improvement consists in utilizing local describing functions together with the global existing ones in the old model (o.m.), as shown in the previous work.[4] Local describing functions are very familiar in the static and dynamic analysis of the structures, if we consider that the classical and currently applied FEM uses these between grid points.

An interesting and sophisticated technique of FEM, commonly called p-convergence elements method,[13] uses grid points on the boundaries of each structural element and series expansions of hierarchic local describing functions, where the coefficients have no physical meaning. The interpolation functions in that approach are both Lagrangian and Hermitian.[10,13]

From a mathematical point of view, these specific techniques, p-convergence elements and proposed method (PM), are very similar. Both use polynomial power series expansions with a degree that can increase indefinitely. However, there is a basic characteristic that distinguishes this method from all of the numerical approaches of FEM: in the PM instead of grid points, we have global describing functions, defined in all of the space containing the structure. Consequently, there exists only one condition, which can be easily satisfied, to guarantee the continuity of the independent variables along the entire structure: the local describing functions vanish at the boundaries between adjacent elements. As in the Ritz method in nonhomogeneous boundary-value problems, there exists a possibility of employing describing functions satisfying homogeneous boundary conditions, together with others that satisfy the true boundary conditions.

With the introduced functions one can determine by an analytical way all of the integrals that appear in the strain and kinetic energy expressions to form the stiffness and mass matrices. The elements of these matrices corresponding to the coefficients only of the global describing functions, which appear also in the o.m. of PM, have been computed in the previous work, where all of the numerical operations have been sufficiently illustrated. Therefore we omitted repeating them again.

By minimizing then the total energy,[9] one reaches the generalized eigenvalue problem, the solution of which is found by three new algorithms F07FDF, F08SEF, and F02FCF of the Numerical Algorithms Group, Inc. (NAG)[14] utility package, where F07FDF computes the Cholesky factorization of the mass matrix, F08SEF reduces a generalized eigenproblem $Az = \lambda Bz$ to the standard form $Cy = \lambda y$, and F02FCF computes the selected eigensolutions.

Rotation Relations and the Local Describing Functions

The rotation relations, previously used and explained,[4] will be briefly recalled. A plate element in the space of the main reference system is shown in Fig. 1.

A local plate reference system x_l, y_l, z_l is introduced, with the axis y_l parallel to the axis y, which is connected with the main reference system x, y, z via the following relations:

$$x_i = x_{oi} + R_{ij} x_{lj}, \qquad i = 1, 2, 3, \quad j = 1, 2, 3 \tag{1a}$$

where

$$x_1 = x, \quad x_2 = y, \quad x_3 = z, \quad x_{o1} = x_o, \quad x_{o2} = y_o$$
$$x_{o3} = z_o, \quad x_{l1} = x_l, \quad x_{l2} = y_l, \quad x_{l3} = z_l \tag{1b}$$

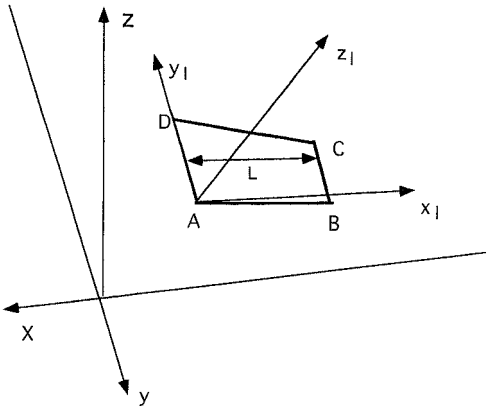

Fig. 1 Plate element in the main reference system x, y, z.

and R_{ij} are the rotation matrix elements. We introduce a nondimensional local coordinates system X_l, Y_l, Z_l:

$$X_l = x_l / L_0, \qquad Y_l = y_l / L_0, \qquad Z_l = z_l / L_0 \tag{2}$$

and $X_{li} = x_{li} / L_0$, where L_0 is a reference length.

Another nondimensional reference system X, Y, Z, which coincides with x, y, z but with a scale factor $1/L_0$, that is, $X = x/L_0$, $Y = y/L_0$, $Z = z/L_0$, and $X_i = x_i/L_0$, is also utilized. Obviously, the two nondimensional reference systems X, Y, Z and X_l, Y_l, Z_l are connected by the same rotation relations (1a). Also the cantilever's plate length L along the axis X_l and the plate thickness h' can be reformulated in nondimensional form, as $\bar{L} = L/L_0$ and $h = h'/L_0$.

By using the rotation relations (1a) and the natural reference system ξ, η,[3,4,15] it is then possible to evaluate the integral:

$$\mathcal{I}_t(i_a, i_b, i_c, i_{ea}, i_{eb}) = \int_S X^{i_a} Y^{i_b} Z^{i_c} X_l^{i_{ea}} Y_l^{i_{eb}} h^t \, \mathrm{d}S, \qquad t = 1, 3 \tag{3}$$

the knowledge of which is necessary to determine the occurring integrals that appear in the expressions of the strain and kinetic energy (see the Appendix).

The displacements u_l, v_l, w_l, along the axes x_l, y_l, z_l, respectively, can be written in terms of the corresponding ones u, v, w along the axes x, y, z, respectively, as

$$u_{li} = R_{ji} u_j, \qquad i = 1, 2, 3, \quad j = 1, 2, 3 \tag{4a}$$

where

$$u_{l1} = u_l, \qquad u_{l2} = v_l, \qquad u_{l3} = w_l$$
$$u_1 = u, \qquad u_2 = v, \qquad u_3 = w \tag{4b}$$

We introduce the nondimensional displacements U, V, W along x, y, z:

$$U = u/L_0, \qquad V = v/L_0, \qquad W = w/L_0 \tag{5}$$

and U_l, V_l, W_l the corresponding ones along x_l, y_l, z_l:

$$U_l = u_l/L_0, \qquad V_l = v_l/L_0, \qquad W_l = w_l/L_0 \tag{6}$$

and $U_{li} = u_{li}/L_0$.

Obviously the relations between U_l, V_l, W_l and U, V, W are the same as in Eq. (4a).

Then the rotations $\theta_X, \theta_Y, \theta_Z$ around the axes y_l, x_l, z_l, respectively, are introduced (the rotation θ_X around y_l is clockwise, whereas the others are anticlockwise), which are connected with the rotations $\theta_x, \theta_y, \theta_z$ around the axes x, y, z, respectively, by the same relations as in Eq. (4a):

$$\theta_{li} = R_{ji} \theta_j, \qquad i = 1, 2, 3, \quad j = 1, 2, 3 \tag{7a}$$

where

$$\theta_{l1} = \theta_Y, \qquad \theta_{l2} = -\theta_X, \qquad \theta_{l3} = \theta_Z$$

$$\theta_1 = \theta_x, \qquad \theta_2 = \theta_y, \qquad \theta_3 = \theta_z \tag{7b}$$

The generic independent variable S_n expression vs the global describing functions, defined in all of the space containing the structure, and the local describing functions, defined only in a single constituting plate element, can be written as

$$S_n = \sum_{i_a i_b i_c} g^{(n)}_{i_a i_b i_c} X^{i_a} Y^{i_b} Z^{i_c} + \sum_{i_{ea} i_{eb}} l^{(I_p)}_{n_{iea,ieb}} X_l^{i_{ea}} Y_l^{i_{eb}} (\bar{L} - \delta_b X_l)$$

$$i_a = 1, 2, \ldots, N_a, \qquad i_b = 0, 1, 2, \ldots, N_b - 1$$

$$i_c = 0, 1, 2, \ldots, N_c - 1 \tag{8a}$$

considering that the clamped edge is supposed at $X = 0$, and

$$i_{ea} = 1, 2, ..N_{ea}, \qquad i_{eb} = 0, 1, 2..N_{eb} - 1$$

$$n_{iea,ieb} = N_{ea} N_{eb} (n - 1) + (i_{ea} - 1) N_{eb} + i_{eb} + 1$$

$$I_p = 1, 2, \ldots, N_{\text{panels}} \tag{8b}$$

where S_n corresponds to U, V, W, θ_x, θ_y, θ_z for $n = 1, 2, \ldots, 6$, respectively, and I_p is the identification number of the generic panel considered, which at most is equal to the total number N_{panels} of panels.

The parameter δ_b is equal to 0 if the edge BC of the plate in Fig. 1 is free, whereas it is equal to 1 if the edge BC lies on a boundary with another adjacent element.

Mathematical Model

The expressions of the strain and kinetic energy, which are well-known,[3,4] depend on products between the independent variables and their first derivatives in the local reference system.

These variables can be transferred into the main reference system by the rotation relations (4a) and (7a), and taking into account the expression (8a), can be written in the form:

$$S_n = \sum_{i_a i_b i_c} g^{(n)}_{i_a i_b i_c} P(i_a, i_b, i_c) + \sum_{i_{ea}, i_{eb}} l^{(I_p)}_{n_{iea,i_{eb}}} e(i_{ea}, i_{eb}) \tag{9a}$$

where

$$P(i_a, i_b, i_c) = X^{i_a} Y^{i_b} Z^{i_c}, \qquad e(i_{ea}, i_{eb}) = X_l^{i_{ea}} (\bar{L} - \delta_b X_l) Y_l^{i_{eb}} \tag{9b}$$

The first derivative of the generic independent variable can be expressed as

$$\frac{\partial S_n}{\partial X_{lu}} = \sum_{i_a i_b i_c} g^{(n)}_{i_a i_b i_c} P_u(i_a, i_b, i_c) + \sum_{i_{ea} i_{eb}} l^{(I_p)}_{n_{iea,i_{eb}}} e_u(i_{ea}, i_{eb})$$

$$u = 1, 2 \tag{10}$$

where from the rotation relations (1a) we have

$$P_u(i_a i_b i_c) = \frac{\partial P(i_a, i_b, i_c)}{\partial X_{lu}} = (i_a \delta_{l1} + i_b \delta_{l2} + i_c \delta_{l3}) R_{iu}$$

$$\times P(i_a - \delta_{l1}, i_b - \delta_{l2}, i_c - \delta_{l3}), \qquad i = 1, 2, 3 \tag{11}$$

and

$$e_u(i_{ea}, i_{eb}) = \frac{\partial e(i_{ea}, i_{eb})}{\partial X_{lu}} = (c_{iu} \bar{L} X_l^{i_{ea} - \delta_{u1}} - \delta_b c_{iu1} X_l^{i_{ea} + 1 - \delta_{u1}}) Y_l^{i_{eb} - \delta_{u2}} \tag{12a}$$

with

$$c_{iu} = [1 + (i_{ea} - 1)\delta_{u1}][1 + (i_{eb} - 1)\delta_{u2}]$$

$$c_{iu1} = (1 + i_{ea}\delta_{u1})[1 + (i_{eb} - 1)\delta_{u2}] \tag{12b}$$

In the expressions of in-plane and out-of-plane flexural-torsional strain energy, there are products between the independent variables first derivatives:

$$\frac{dS_r}{dX_{lu}} \frac{dS_s}{dX_{lv}} = \sum_{i_a i_b i_c} \sum_{j_a j_b j_c} g^{(r)}_{i_a i_b i_c} g^{(s)}_{j_a j_b j_c} P_u(i_a, i_b, i_c) P_v(j_a, j_b, j_c)$$

$$+ \sum_{i_a i_b i_c} \sum_{i_{ea} i_{eb}} \Big[g^{(r)}_{i_a i_b i_c} l^{(I_p)}_{s_{jea,j_{eb}}} P_u(i_a i_b i_c) e_v(j_{ea}, j_{eb})$$

$$+ l^{(I_p)}_{r_{iea,i_{eb}}} g^{(s)}_{j_a j_b j_c} e_u(i_{ea}, i_{eb}) P_v(j_a j_b j_c) \Big]$$

$$+ \sum_{i_{ea} i_{eb}} \sum_{j_{ea} j_{eb}} l^{(I_p)}_{r_{iea,i_{eb}}} l^{(I_p)}_{s_{jea,j_{eb}}} e_u(i_{ea}, i_{eb}) e_v(j_{ea}, j_{eb})$$

$$r, s = 1, 2, 3 \longrightarrow \text{in-plane}, \qquad r, s = 4, 5, 6 \longrightarrow \text{out-of-plane}$$

$$u, v = 1, 2 \tag{13}$$

In the out-of-plane shear-strain energy expression there are products between independent variables and their first derivatives, such as

$$\frac{\partial S_r}{\partial X_{lu}} S_s = \sum_{i_a i_b i_c} \sum_{j_a j_b j_c} g^{(r)}_{i_a i_b i_c} g^{(s)}_{j_a j_b j_c} P_u(i_a, i_b, i_c) P(j_a, j_b, j_c)$$

$$+ \sum_{i_a i_b i_c} \sum_{i_{ea} i_{eb}} \Big[g^{(r)}_{i_a i_b i_c} l^{(I_p)}_{s_{jea,j_{eb}}} P_u(i_a i_b i_c) e(j_{ea}, j_{eb})$$

$$+ l^{(I_p)}_{r_{iea,i_{eb}}} g^{(s)}_{j_a j_b j_c} e_u(i_{ea}, i_{eb}) P(j_a, j_b, j_c) \Big]$$

$$+ \sum_{i_{ea} i_{eb}} \sum_{j_{ea} j_{eb}} l^{(I_p)}_{r_{iea,i_{eb}}} l^{(I_p)}_{s_{jea,j_{eb}}} e_u(i_{ea}, i_{eb}) e(j_{ea}, j_{eb})$$

$$r = 1, 2, 3, \quad s = 4, 5, 6, \quad u = 1, 2 \tag{14}$$

and its dual expression:

$$S_r \frac{\partial S_s}{\partial X_{lv}} = \sum_{i_a i_b i_c} \sum_{j_a j_b j_c} g^{(r)}_{i_a i_b i_c} g^{(s)}_{j_a j_b j_c} P(i_a, i_b, i_c) P_v(j_a, j_b, j_c)$$

$$+ \sum_{i_a i_b i_c} \sum_{i_{ea} i_{eb}} \Big[g^{(r)}_{i_a i_b i_c} l^{(I_p)}_{s_{jea,j_{eb}}} P(i_a i_b i_c) e_v(j_{ea}, j_{eb})$$

$$+ l^{(I_p)}_{r_{iea,i_{eb}}} g^{(s)}_{j_a j_b j_c} e(i_{ea}, i_{eb}) P_v(j_a j_b j_c) \Big]$$

$$+ \sum_{i_{ea} i_{eb}} \sum_{j_{ea} j_{eb}} l^{(I_p)}_{r_{iea,i_{eb}}} l^{(I_p)}_{s_{jea,j_{eb}}} e(i_{ea}, i_{eb}) e_v(j_{ea}, j_{eb})$$

$$r = 4, 5, 6, \quad s = 1, 2, 3, \quad v = 1, 2 \tag{15}$$

In the out-of-plane shear-strain and kinetic-energy expressions, products between independent variables appear, as shown:

$$S_r S_s = \sum_{i_a i_b i_c} \sum_{j_a j_b j_c} g^{(r)}_{i_a i_b i_c} g^{(s)}_{j_a j_b j_c} P(i_a, i_b, i_c) P(j_a, j_b, j_c)$$

$$+ \sum_{i_a i_b i_c} \sum_{i_{ea} i_{eb}} \Big[g^{(r)}_{i_a i_b i_c} l^{(I_p)}_{s_{jea,j_{eb}}} P(i_a i_b i_c) e(j_{ea}, j_{eb})$$

$$+ l^{(I_p)}_{r_{iea,i_{eb}}} g^{(s)}_{j_a j_b j_c} e(i_{ea}, i_{eb}) P(j_a, j_b, j_c) \Big]$$

$$+ \sum_{i_{ea} i_{eb}} \sum_{j_{ea} j_{eb}} l^{(I_p)}_{r_{iea,i_{eb}}} l^{(I_p)}_{s_{jea,j_{eb}}} e(i_{ea}, i_{eb}) e(j_{ea}, j_{eb})$$

$$r, s = 1, 2, 3 \longrightarrow \text{displacements}, \qquad r, s = 4, 5, 6 \longrightarrow \text{rotations} \tag{16}$$

In Eqs. (13–16) the first terms on the right-hand side give the contributions due only to the global describing functions, previously considered in the o.m.[4] New contributions are brought by the coupling between global and local functions, as the second and third terms (the one of which is the dual of the other), and only by the local describing functions, as the fourth terms.

Thus the strain energy expression can be determined vs the Lagrangian degrees of freedom and written in the classical form:

$$\mathcal{U}_T = \frac{1}{2} \sum_{ij} k_{ij} q_i q_j \tag{17}$$

where k_{ij} are the elements of the stiffness matrix K (see the Appendix) and the generalized degree of freedom (DOF) q_i, if we refer to the series expansion (9a), can be defined as follows:

$$q_i = g^{(n)}_{i_a i_b i_c} \tag{18a}$$

for

$$i \leq N^*, \qquad N^* = 6N_a N_b N_c \tag{18b}$$

and

$$i = (i_a - 1)N_b N_c + i_b N_c + i_c + (n-1)(N^*/6) + 1 \tag{18c}$$

as in the o.m., whereas for

$$N^* < i \leq N \tag{18d}$$

we have

$$q_i = l^{(I_p)}_{n_{iea,ieb}} \tag{18e}$$

and

$$i = N^* + (I_p - 1)6N_{ea}N_{eb} + n_{iea,ieb} \tag{18f}$$

Also the total kinetic energy can be expressed vs the Lagrangian DOF, as

$$\mathcal{T} = \frac{1}{2}\omega^2 \sum_{ij} m_{ij} q_i q_j \tag{19}$$

where m_{ij} are the elements of the mass matrix M (see the Appendix). At last, by minimizing the total energy,[7–9] we arrive at the generalized eigenvalue problem:

$$(K - \omega^2 M)Q = 0 \tag{20}$$

the solution of which is found by appropriate algorithms.

Applications

Two new different cases of multipanel aircraft structures in a three-dimensional space have been considered. The internal structure of the vibrating panels now is the same of the cases previously examinated for the o.m. application,[4] with a linear chordwise variation of the thickness. Its value at the trailing edge is twice the one at the leading edge.

The first case refers to a wing structure as in Fig. 2, with four component elements. The first couple of them lie on the aircraft plane, the third one is a little inclined with respect to them, whereas the fourth element with higher inclination, at the end of the spanwise wing structure, could be a typical winglet.

In Fig. 2a the flattened structure is sketched, whereas the true positioning of the plates in a three-dimensional space is shown in Fig. 2b. A sample of the grid mesh, corresponding to $N = 828$, is depicted in Fig. 2c.

A tail structure with three component elements identical to the ones previously utilized for the o.m. application,[4] but with an added fourth vertical element above the horizontal control surfaces (containing the pitch elevators), which is useful to increase the aircraft

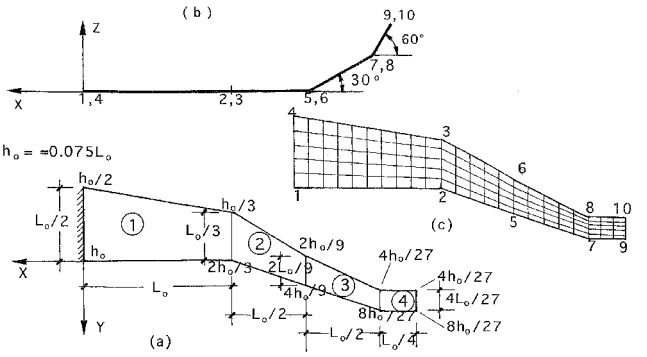

Fig. 2 Wing structure: a) flattened wing structure in the first case, b) true positioning of the plates, and c) a grid mesh of the utilized FEM model.

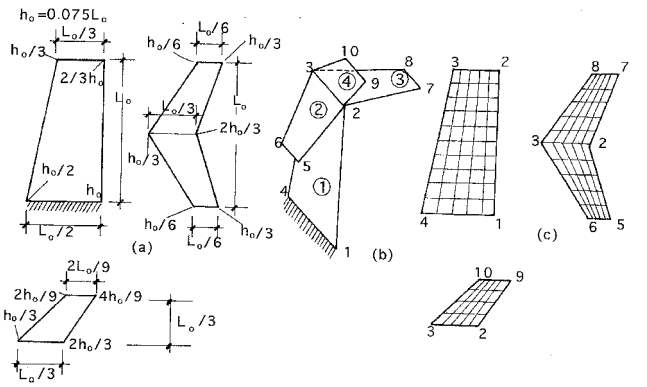

Fig. 3 Tail structure in the second case considered, together with c) a grid mesh of the FEM model.

lateral stability, is then analyzed. All of the component plate elements are sketched in Fig. 3a, and a trimetric view of the same structure in a threedimensional space is shown in Fig. 3b. A sample of the grid mesh, corresponding to $N = 864$, is depicted in Fig. 3c.

Results

The tables show the values of the nondimensional frequency parameter

$$\omega_d^2 = \omega^2(\rho L_0^2 / E)$$

The results obtained by both models of PM from the dynamic analysis of the tail structure, previously considered for the o.m. application,[4] are shown in Table 1. Table 2 shows the numerical test matrix of both models, which specifies the number of global and local describing functions coefficients vs the number N of Lagrangian DOF. The reason that the CPU times requested by the o.m. are much smaller than the corresponding ones in the previous work[4] is that three more efficient numerical eigensolver algorithms are used instead of the old F02BJf of the NAG utility package.[14] Unfortunately, these new algorithms are not able to eliminate the convergence problems, for which is not possible to increase the number N of DOF beyond $N = 360$, because no reliable results can be obtained over such a limit.

We can notice that the values (CV) toward which both the PM and FEM results converge approximately, which were obtained by polynomial extrapolation with the o.m.,[4] can be obtained by numerical way with this new model (n.m.).

The results of FEM and also the modal shapes of this particular tail structure have been already determined and shown in the previous work,[4] and consequently it is not necessary to report them again.

Then the results of the two new cases have to be examinated. Table 3 refers to the first one with a multipanel composed wing

Table 1 Vibration frequencies obtained in a previously considered case

Numerical parameters	PM (o.m.)		PM (n.m.)			CV
N	300	360	924	936	948	——
CPU s.	5.42	8.01	36.25	44.64	55.03	——
First VM	0.03758	0.03757	0.03756	0.03756	0.03756	0.03756
Second VM	0.1022	0.1021	0.1021	0.1020	0.1020	0.1020
Third VM	0.1176	0.11757	0.1176	0.1175	0.1175	0.1175

Table 2 PM numerical test matrix in a previously considered case

N	N_a	N_b	N_c	N_{ea}	N_{eb}
			n.m.		
924	1	10	1	6	6
936	1	12	1	6	6
948	1	14	1	6	6
			o.m.		
300	5	5	2	——	——
360	5	6	2	——	——

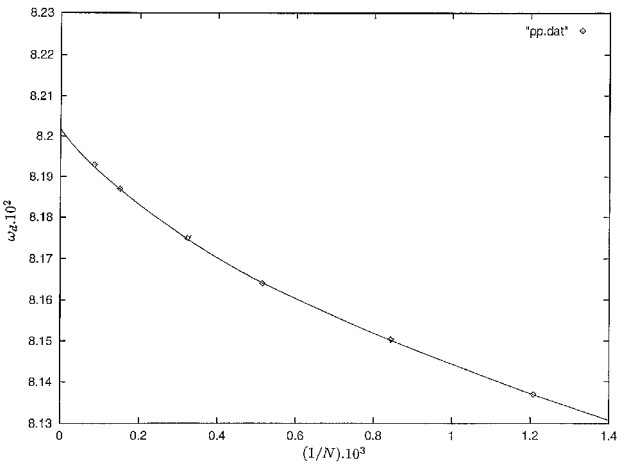

Fig. 4 Behavior of the third frequency obtained by the FEM vs 1/*N* in the first case considered.

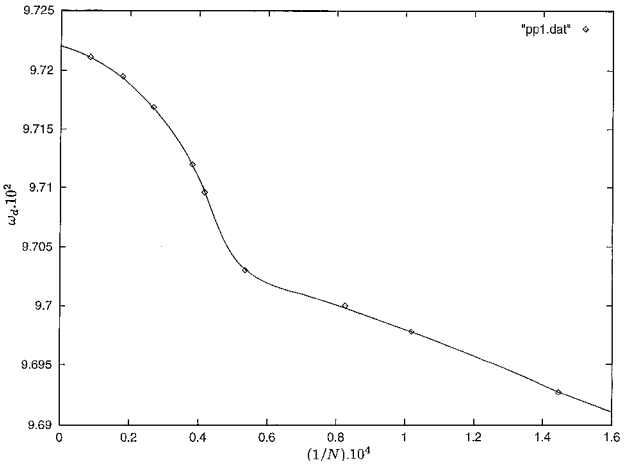

Fig. 5 Behavior of the second frequency obtained by the FEM vs 1/*N* in the second case considered.

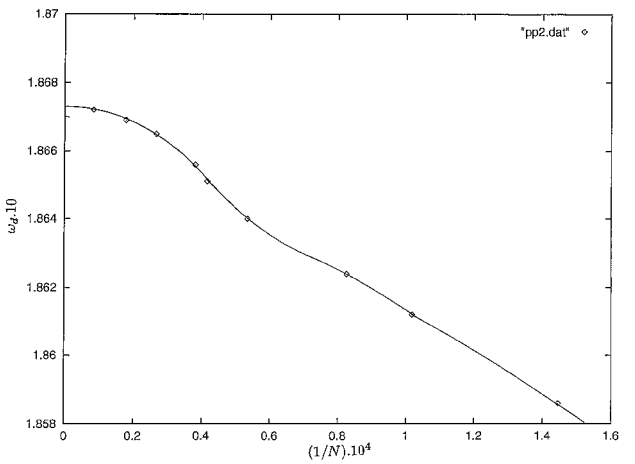

Fig. 6 Behavior of the fourth frequency obtained by the FEM vs 1/*N* in the second case considered.

structure. The frequency values indicated have been obtained both by the PM and the FEM, using a MSC/NASTRAN[16] program (version 70 and with lumped-mass formulation). The bidimensional plate elements used in the MSC/NASTRAN program are QUAD4, with linear isoparametric variation of the thickness over their surfaces.

The FEM numerical test matrix that specifies the number of elements into which all of the plate component elements are divided, spanwise and chordwise, with their indicative number, is reported in Table 4. In Table 4 the PM (n.m.) numerical test matrix is shown, whereas the corresponding one of the o.m. is written in Table 2.

The frequency results of PM (n.m.) converge very quickly toward their limit values, and for this reason it is not necessarily a graphical test of their behavior vs $1/N$. Also, the values obtained by FEM converge quickly toward those of PM, except the third frequency of the first torsional vibrating mode, for which it is useful to look at the Fig. 4, which gives its behavior vs $1/N$. The data points, corresponding to the results of Table 3 obtained by FEM, appear in Fig. 4 as dots. From a careful analysis one can notice that it converges approximately toward the corresponding value obtained by the PM (n.m.).

Table 5 shows the same frequency parameter values in the second case with a tail structure. The FEM and PM (n.m.) numerical test matrices are shown in Table 6, whereas the corresponding one of the PM (o.m.) is the same as Table 2. The first and third frequency values of FEM converge quickly toward the corresponding ones of PM (n.m), whereas for the two other frequencies it is useful to have an insight into their behavior vs $1/N$, as in Figs. 5 and 6. One can notice that they converge approximately toward the same values of PM. In the preceding figures all of the data points that appear as dots correspond to the FEM results of Table 5 from $N = 6912$ and over.

The modal shapes obtained by both methods have to be considered. They have been obtained by dividing the plate component elements as in the grid mesh shown in Fig. 2c in the first case and in Fig. 3c in the second case. In the same grid points of the FEM model, the displacements values along the three axes of the main reference system have been computed by the decribing functions utilized in the PM (n.m.), and the modal shapes have been built for a comparison with the ones of FEM.

In Fig. 7, a trimetric view of the undeformed wing structure grid mesh, the elements of which are reported in Fig. 2c, is sketched, whereas Figs. 8–11 show the modal shapes obtained by the FEM a) with $N = 828$ and the PM (n.m.) b) with $N = 528$. In Fig. 12,

Table 3 Vibration frequencies obtained in the first case

Numerical parameters	PM (o.m.)		PM (n.m.)			FEM					
N	300	360	528	546	564	828	1176	1944	3036	6624	11592
CPU s.	6.89	9.70	28.36	33.79	40.83	8.5	10.8	13.8	18.4	40.6	67.6
First VM	0.01995	0.01994	0.01993	0.01993	0.01993	0.01987	0.01989	0.01991	0.01992	0.01993	0.01993
Second VM	0.0562	0.05059	0.05058	0.05058	0.05058	0.05040	0.05049	0.05054	0.05057	0.05058	0.05058
Third VM	0.08210	0.08206	0.08206	0.08203	0.08202	0.08137	0.08151	0.08164	0.08176	0.08187	0.08193
Fourth VM	0.1213	0.1210	0.1208	0.1208	0.1208	0.1204	0.1206	0.1207	0.1207	0.1208	0.1208

Table 4 FEM and PM (n.m.) numerical test matrix in the first case

FEM						PM					
N	Span.1	Span.2	Span.3	Span.4	Chord.	N	N_a	N_b	N_c	N_{ea}	N_{eb}
828	10	5	5	3	5	528	3	8	1	4	4
1,176	12	6	6	4	6	546	3	9	1	4	4
1,944	15	8	8	5	8	564	3	10	1	4	4
3,036	20	10	10	6	10	——	——	——	——	——	——
6,624	30	15	15	9	15	——	——	——	——	——	——
11,592	40	20	20	12	20	——	——	——	——	——	——

Table 5 Vibration frequencies obtained in the second case

Numerical parameters	PM (o.m.)		PM (n.m.)			FEM										
N	300	360	924	936	948	864	3,168	6,912	9,804	12,096	18,720	24,024	26,208	37,440	56,160	112,320
CPU s	——	17.95	64.55	76.94	92.41	8.7	19.1	36.0	55.6	62.6	94.9	120.7	131.5	195.2	284.0	587.7
First VM	0.03168	0.03160	0.03158	0.03158	0.03158	0.03145	0.03155	0.03156	0.03157	0.03157	0.03157	0.03157	0.03158	0.03158	0.03158	0.03158
Second VM	0.09734	0.09728	0.09724	0.09723	0.09722	0.09507	0.09668	0.09693	0.09698	0.09700	0.09703	0.097096	0.09712	0.097169	0.097195	0.09721
Third VM	0.1168	0.1166	0.1164	0.1164	0.1164	0.1144	0.1159	0.1161	0.1162	0.1162	0.1163	0.1163	0.1163	0.1163	0.1163	0.1164
Fourth VM	0.18684	0.18678	0.18678	0.18676	0.18674	0.1790	0.1848	0.18586	0.18612	0.18624	0.1864	0.18651	0.18656	0.18665	0.18669	0.18672

Table 6 FEM and PM (n.m.) numerical test matrix in the second case

FEM						PM					
N	Span.1	Span.2	Span.3	Span.4	Chord.	N	N_a	N_b	N_c	N_{ea}	N_{eb}
864	10	5	5	4	5	924	1	10	1	6	6
3,168	20	10	10	8	10	936	1	12	1	6	6
6,912	30	15	15	12	15	948	1	14	1	6	6
9,804	36	18	18	14	18	——	——	——	——	——	——
12,096	40	20	20	16	20	——	——	——	——	——	——
18,720	50	25	25	20	25	——	——	——	——	——	——
26,208	70	35	35	28	25	——	——	——	——	——	——
37,440	100	50	50	40	25	——	——	——	——	——	——
56,150	150	75	75	60	25	——	——	——	——	——	——
112,320	300	150	150	120	25	——	——	——	——	——	——

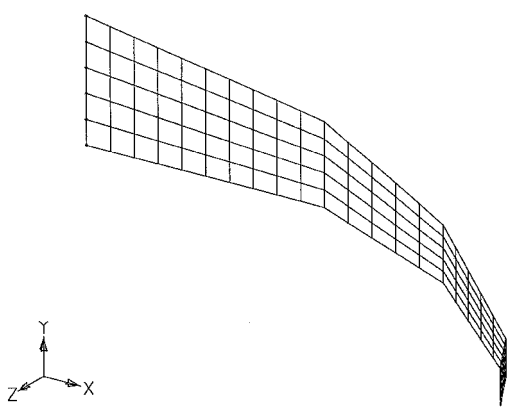

Fig. 7 Trimetric view of the undeformed wing structure grid mesh in the first case considered.

a trimetric view of the undeformed tail structure grid mesh, the elements of which are reported in Fig. 3c, is depicted, whereas Figs. 13–16 show the modal shapes obtained by the FEM a) with $N = 864$ and the PM (n.m.) b) with $N = 924$.

The reason for which in the same figure the undeformed structure grid mesh together with the modal shape appear is that it is easier to characterize the form of the vibrating-mode (VM) shape by looking at the displacements of the grid points in the main reference system. One could notice a good agreement between the modal shapes of the two methods.

Discussion

Now the obtained results will be discussed, and the reason for chosing these wing and tail structures will be explained. In both cases, one can emphasize higher convergence rate of this PM if the n.m. is used, both for lesser CPU time and a lower number N of Lagrangian DOF. However, another important fact has to be remarked. The second case shows a higher complexity of the structure because a couple of elements lie on a plane perpendicular to the others.

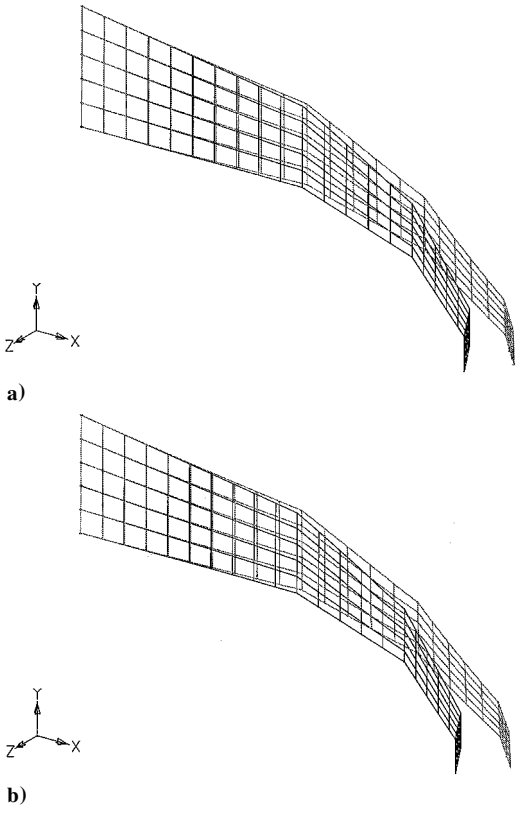

Fig. 8 First flexural mode shape corresponding to the first frequency, obtained in the first case: a) by the FEM with $N = 828$ and b) by the PM with $N = 528$.

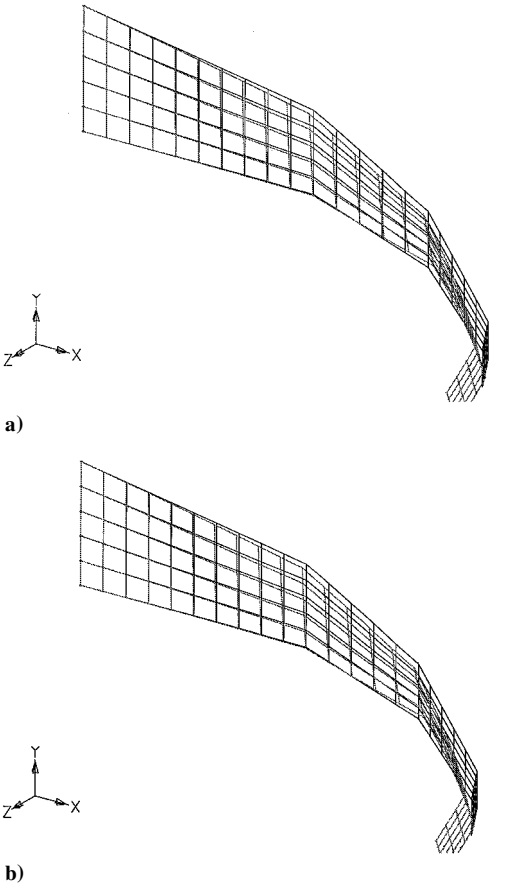

Fig. 10 First torsional mode shape corresponding to the third frequency, obtained in the first case: a) by the FEM with $N = 828$ and b) by the PM with $N = 528$.

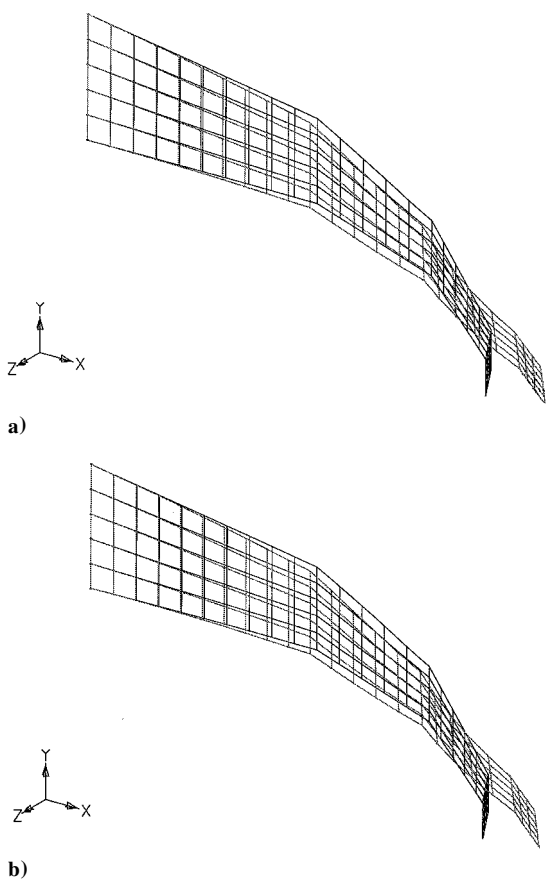

Fig. 9 Second flexural mode shape corresponding to the second frequency, obtained in the first case: a) by the FEM with $N = 828$ and b) by the PM with $N = 528$.

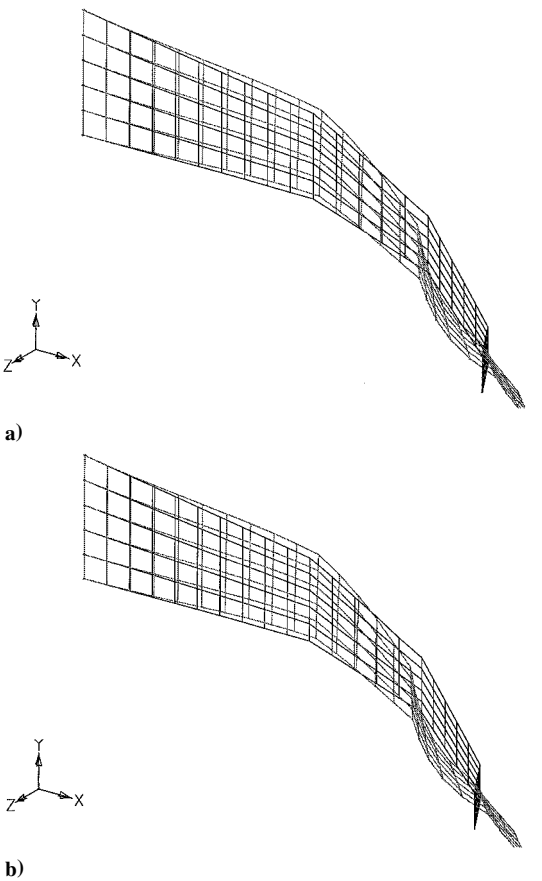

Fig. 11 Third flexural mode shape corresponding to the fourth frequency, obtained in the first case: a) by the FEM with $N = 828$ and b) by the PM with $N = 528$.

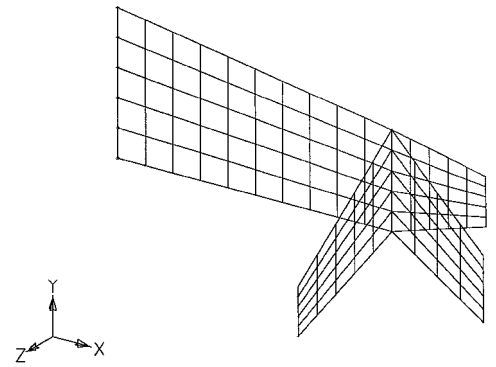

Fig. 12 Trimetric view of the undeformed tail structure grid mesh in the second case considered.

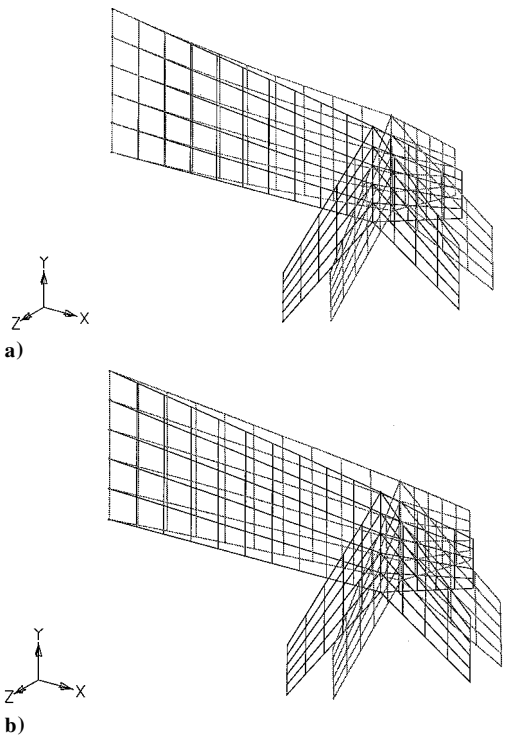

Fig. 13 First flexural mode shape corresponding to the first frequency, obtained in the first case: a) by the FEM with $N = 864$ and b) by the PM with $N = 924$.

If the FEM is used in the first case, $N = 11592$ and a CPU time of 67.6 s. are sufficient to obtain for the first torsional mode frequency (third VM) nearly as an accurate value as the corresponding one of the first torsional mode frequency (second VM) in the second case with $N = 26208$ and a CPU time of 131.5 s. Further, in the first case $N = 6624$ and a CPU time of 40.6 s. are sufficient to obtain for the fourth frequency a value coincident with the same of PM (n.m.), whereas in the second case an enormous number N of Lagrangian DOF and a CPU time of 587.7 s. are necessary to obtain a value of the fourth frequency nearly coincident with the same of PM (n.m.), that is, the requested number of DOF and CPU time to have accurate values increase with FEM a lot more than with PM, when we pass from the first to the second case. With this n.m. of PM, we can save both core storage requirements and CPU time as the complexity of the structure grows indefinitely.

Furthermore, these advantages become more obvious if higher-order vibration modes are requested because the CPU time of the MSC/NASTRAN program increases with the number of eigensolutions required much more than the corresponding time of PM. The number N of DOF grows much more, too.

Unfortunately accurate frequency values cannot be obtained by the o.m. of PM because of convergence problems, which become more limitating with the increasing structure complexity.

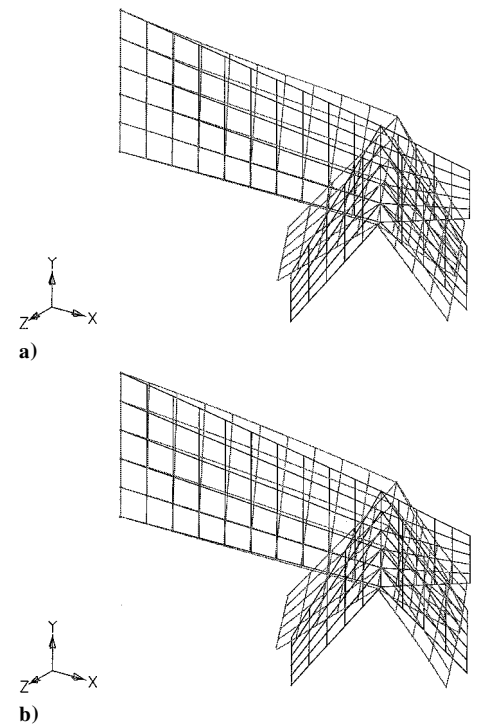

Fig. 14 First torsional mode shape corresponding to the second frequency, obtained in the second case: a) by the FEM with $N = 864$ and b) by the PM with $N = 924$.

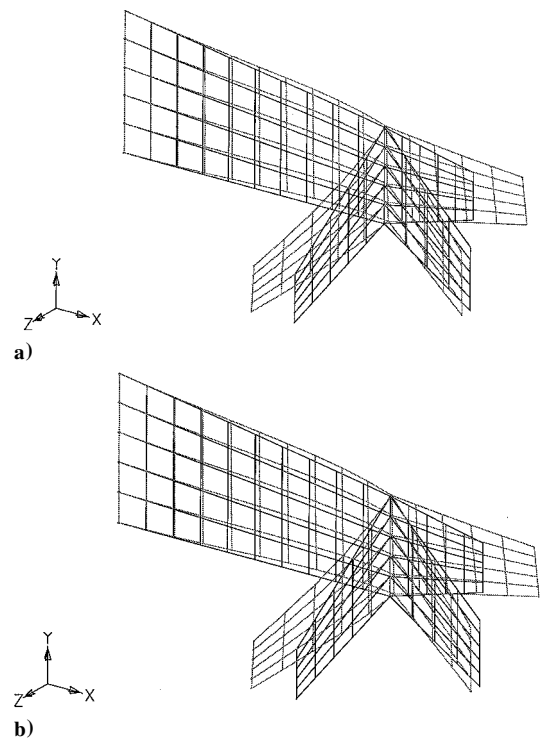

Fig. 15 Second flexural mode shape corresponding to the third frequency, obtained in the second case: a) by the FEM with $N = 864$ and b) by the PM with $N = 924$.

There are also disadvantages caused by the presence of spurious solutions particularly in this n.m., for which the eigensolver algorithms waste some of the CPU time to search these unwanted guests.

Moreover there are limits of applicability also of this n.m. because, like in the o.m., the bidimensional component panels in a three-dimensional space are considered as plates in a monolithic fashion with homogeneous and isotropic constituting material and based on the Mindlin[17,18] theory for the shear behavior. This is not very realistic considering that the usual mode of construction

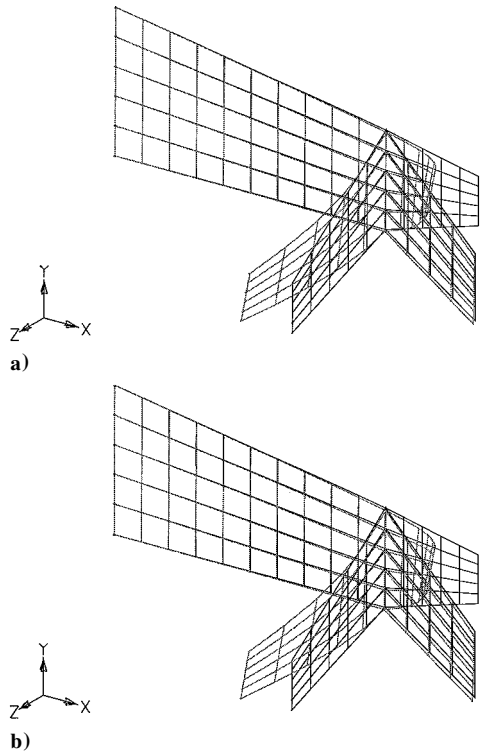

Fig. 16 Third flexural mode (symmetric) shape corresponding to the fourth frequency, obtained in the second case: a) by the FEM with N = 864 and b) by the PM with N = 924.

of the aircraft structures is the semimonocoque stiffened shell form.

Future and more sophisticated eigensolver algorithms will allow the saving of the CPU time wasted to find the spurious solutions.

Further more realistic plate models, similar to the ones introduced by Giles[19,20] and Livne[21–23] for planform wing structures with general geometry, such as cranked boxes, will allow the application of this method to true cases of multipanel aircraft structures in a three-dimensional space, also with nonlinear chordwise thickness variation.

Conclusions

The effects of the improvement of the utilized model of PM are evident from a simple analysis of the obtained results. The o.m. appears to be excellent for a limited number of component elements of the structures, but gives less accurate frequency values if the complexity of the structure grows indefinitely because of convergence problems. However, such limits can be overcome by using this n.m.

Further implementation of the numerical program of the introduced procedure is necessary, considering that only idealized plate models for the component panels of the structures have been utilized. Future applications of this method with a more realistic way of modeling the true internal structure of the flat component elements will allow it to obtain interesting results for practical utilization.

We can conclude by saying that this alternative procedure to FEM offers high accuracy, based on the results obtained.

Appendix: Evaluation of the Stiffness and Mass Matrices

In this paper only the integrals where local describing functions appear will be taken into account because the others with only global describing functions have already been introduced and evaluated.[4]

In the expressions (13–16) only the first of the two terms of the coupling between global and local describing functions for the moment will be considered because the effect of its dual one will be evaluated when the symmetry of both stiffness and mass matrices is imposed.

We introduce the integrals:

$$P_{et}(i_a, i_b, i_c, j_{ea}, j_{eb}) = \int_S P(i_a, i_b, i_c)e(j_{ea}, j_{eb})h^t \, dS \qquad t = 1, 3 \quad \text{(A1)}$$

$$P_{ue}(i_a, i_b, i_c, j_{ea}, j_{eb}) = \int_S P_u(i_a, i_b, i_c)e(j_{ea}, j_{eb})h \, dS \qquad u = 1, 2 \quad \text{(A2)}$$

$$P_{ev}(i_a, i_b, i_c, j_{ea}, j_{eb}) = \int_S P(i_a, i_b, i_c)e_v(j_{ea}, j_{eb})h \, dS \qquad v = 1, 2 \quad \text{(A3)}$$

$$P_{uevt}(i_a, i_b, i_c, j_{ea}, j_{eb}) = \int_S P_u(i_a, i_b, i_c)e_v(j_{ea}, j_{eb})h^t \, dS \qquad u, v = 1, 2, \quad t = 1, 3 \quad \text{(A4)}$$

$$e_{et}(i_{ea}, i_{eb}, j_{ea}, j_{eb}) = \int_S e(i_{ea}, i_{eb})e(j_{ea}, j_{eb})h^t \, dS \qquad t = 1, 3 \quad \text{(A5)}$$

$$e_{ue}(i_{ea}, i_{eb}, j_{ea}, j_{eb}) = \int_S e_u(i_{ea}, i_{eb})e(j_{ea}, j_{eb})h \, dS \qquad u = 1, 2 \quad \text{(A6)}$$

$$e_{uvt}(i_{ea}, j_{ea}, i_{eb}, j_{eb}) = \int_S e_u(i_{ea}, i_{eb})e_v(j_{ea}, j_{eb})h^t \, dS \qquad u, v = 1, 2, \quad t = 1, 3 \quad \text{(A7)}$$

Now the stiffness and mass matrices can be determined. All of the elements corresponding to the coefficients only of the global describing functions, which appear also in the o.m. of PM, are not computed in this paper because they have already been evaluated.[4] All of the just-mentioned integrals will be used.

First it is necessary to recall six couples of subscripts i_r, i_s, already introduced and used in the o.m.,[4] corresponding to the coefficients of the global describing functions of the independent variables U, V, W, θ_x, θ_y, θ_z for r, s = 1.2...6, respectively. From the relations (18a) and (18c) we can write

$$q_{i_r} = g^{(r)}_{i_a i_b i_c}, \qquad q_{j_s} = g^{(s)}_{j_a j_b j_c}, \qquad r, s = 1, 2...6 \quad \text{(A8)}$$

where

$$i_r = (i_a - 1)N_b N_c + i_b N_c + i_c + (r - 1)(N^*/6) + 1$$

$$j_s = (j_a - 1)N_b N_c + j_b N_c + j_c + (s - 1)(N^*/6) + 1 \quad \text{(A9)}$$

Then six new couples of subscripts i_{er}, j_{es}, corresponding to the coefficients of the local describing functions of the same independent variables for $r, s = 1, 2...6$, respectively, have to be introduced. We have from the relations (18e)

$$q_{i_{er}} = l^{(I_p)}_{r_{iea,ieb}}, \qquad q_{j_{es}} = l^{(I_p)}_{s_{jea,jeb}}, \qquad r, s = 1, 2, \ldots, 6 \quad \text{(A10)}$$

where from the expressions (8b)

$$r_{iea,ieb} = N_{ea}N_{eb}(r - 1) + (i_{ea} - 1)N_{eb} + i_{eb} + 1$$

$$s_{jea,jeb} = N_{ea}N_{eb}(s - 1) + (j_{ea} - 1)N_{eb} + j_{eb} + 1$$

$$i_{ea}, j_{ea} = 1, 2, \ldots, N_{ea}, \quad i_{eb}, j_{eb} = 0, 1, 2, \ldots, N_{eb} - 1$$

$$r, s = 1, 2, \ldots, 6 \quad \text{(A11)}$$

and consequently from the relations (18f) one obtains

$$i_{er} = N^* + (I_p - 1)6N_{ea}N_{eb} + r_{iea,ieb}$$

$$j_{es} = N^* + (I_p - 1)6N_{ea}N_{eb} + s_{jea,jeb} \qquad \text{(A12)}$$

Thus the mixed elements of the stiffness matrix, which arise from the coupling between global and local describing functions, can be evaluated. If the series expansions (9a) are substituted into the out-of-plane and in-plane strain energy expressions,[4] taking into account the rotation relations (4a) and (7a), and the first one of the two coupling terms on the right-hand side of Eqs. (13–17), and using the integrals (A2–A4), the corresponding stiffness matrix elements are determined:

$$\begin{aligned} k_{i_r j_{es}} &= E_{12}L_0^3[R_{r-3,2}R_{s-3,2}(P_{1e13} + \nu_{12}P_{2e23}) \\ &\quad - R_{r-3,2}R_{s-3,1}(\nu_{12}P_{2e13} + \nu P_{1e23}) - R_{r-3,1}R_{s-3,2}(\nu_{12}P_{1e23} \\ &\quad + \nu P_{2e13}) + R_{r-3,1}R_{s-3,1}(P_{2e23} + \nu_{12}P_{1e13})] \\ &\quad + GL_0^3[(R_{r-3,2}R_{s-3,2} + R_{r-3,1}R_{s-3,1}]P_{e1} \end{aligned}$$

$$r, s = 4, 5, 6 \qquad \text{(A13)}$$

where

$$\nu_{12} = (1 - \nu)/2, \qquad E_{12} = [E/12(1 - \nu^2)]$$

$$\begin{aligned} k_{i_r j_{es}} &= GL_0^3R_{r3}R_{s3}(P_{1e11} + P_{2e21}) \\ &\quad + AL_0^3[R_{r1}R_{s1}(P_{1e11} + \nu_{12}P_{2e21}) + R_{r1}R_{s2}(\nu_{12}P_{2e11} + \nu P_{1e21}) \\ &\quad + R_{r2}R_{s1}(\nu_{12}P_{1e21} + \nu P_{2e11}) + R_{r2}R_{s2}(P_{2e21} + \nu_{12}P_{111})] \end{aligned}$$

$$r, s = 1, 2, 3 \qquad \text{(A14)}$$

where

$$A = E/(1 - \nu^2)$$

$$k_{i_r j_{es}} = -GL_0^3(-R_{r3}R_{s-3,2}P_{1e} + R_{r,3}R_{s-3,1}P_{2e})$$

$$r = 1, 2, 3, \quad s = 4, 5, 6 \qquad \text{(A15)}$$

$$k_{i_r j_{es}} = -GL_0^3(-R_{r-3,2}R_{s3}P_{e1} + R_{r-3,1}R_{s,3}P_{e2})$$

$$r = 4, 5, 6, \quad s = 1, 2, 3 \qquad \text{(A16)}$$

If the series expansions (9a) are substituted into the expression of the kinetic energy[4] and taking into account the first of the two coupling terms on the right-hand side of Eq. (16) and the integral (A1), we can determine the mass matrix mixed elements

$$m_{i_r j_{er}} = \rho L_0^5 P_{e1}, \qquad r = 1, 2, 3 \qquad \text{(A17)}$$

$$m_{i_r j_{er}} = (\rho L_0^5/12)P_{e3}, \qquad r = 4, 5, 6 \qquad \text{(A18)}$$

At last the contributions caused only by the local describing functions have to be considered. If the local describing functions of the series expansions (9a) are substituted into the out-of-plane and in-plane strain energy expressions,[4] the corresponding stiffness matrix elements can be determined. This takes into account the integrals (A6) and (A7), the rotation relations (4a) and (7a), and the fourth terms on the right-hand side of Eqs. (13), (14), and (16). The contribution of the Eq. (15), dual of Eq. (14), will be taken into account when the stiffness matrix symmetry is imposed. Thus we have

$$\begin{aligned} k_{ier\,jes} &= E_{12}L_0^3[R_{r-3,2}R_{s-3,2}(e_{113} + \nu_{12}e_{223}) \\ &\quad - R_{r-3,2}R_{s-3,1}(\nu_{12}e_{213} + \nu e_{123}) \\ &\quad - R_{r-3,1}R_{s-3,2}(\nu_{12}e_{123} + \nu e_{213}) + R_{r-3,1}R_{s-3,1}(e_{223} \\ &\quad + \nu_{12}e_{113})] + GL_0^3(R_{r-3,2}R_{s-3,2} + R_{r-3,1}R_{s-3,1})e_{e1} \end{aligned}$$

$$r, s = 4, 5, 6, \quad r \le s \qquad \text{(A19)}$$

$$\begin{aligned} k_{ier\,jes} &= GL_0^3R_{r3}R_{s3}(e_{111} + e_{221}) + E_\nu L_0^3[R_{r1}R_{s1}(e_{111} + \nu_{12}e_{221}) \\ &\quad + R_{r1}R_{s2}(\nu_{12}e_{211} + \nu e_{121}) + R_{r2}R_{s1}(\nu_{12}e_{121} + \nu e_{211}) \\ &\quad + R_{r2}R_{s2}(e_{221} + \nu_{12}e_{111})], \end{aligned}$$

$$r, s = 1, 2, 3, \quad r \le s \qquad \text{(A20)}$$

$$k_{ier\,jes} = -GL_0^3[-R_{r3}R_{s-3,2}e_{1e} + R_{r,3}R_{s-3,1}e_{2e}]$$

$$r = 1, 2, 3, \quad s = 4, 5, 6 \qquad \text{(A21)}$$

If the local describing functions of the series expansions (9a) are substituted into the kinetic energy expression,[4] and taking into account the fourth term on the right-hand side of Eq. (16) and the integral (A5), we can determine the mass matrix elements

$$m_{i_{er}j_{er}} = \rho L_0^5 e_{e1}, \qquad r = 1, 2, 3 \qquad \text{(A22)}$$

$$m_{i_{er}j_{er}} = (\rho L_0^5/12)e_{e1}, \qquad r = 4, 5, 6 \qquad \text{(A23)}$$

At last the symmetry of both stiffness and mass matrices has to be imposed, thus also the dual elements of the ones already determined can be evaluated:

$$k_{ji} = k_{ij} \qquad \text{(A24)}$$

$$m_{ji} = m_{ij} \qquad \text{(A25)}$$

$$i = 1, N - 1, \qquad j = i + 1, N$$

Acknowledgments

The author is grateful to Antonio Paolozzi of the Aerospace Department of the University of Rome "La Sapienza" for his precious collaboration.

References

[1]Tizzi, S., "A Numerical Procedure for the Analysis of a Vibrating Panel in Critical Flutter Conditions," *Computers and Structures*, Vol. 50, No. 3, 1994, pp. 299–316.

[2]Juanky, N., Knight, N. F. Jr., and Ambur, D. R., "Buckling of Arbitrary Quadriteral Anisotropic Plates," *AIAA Journal*, Vol. 33, No. 5, 1995, pp. 938–944.

[3]Tizzi, S., "Application of a Numerical Procedure for the Dynamic Analysis of Plane Aeronautical Structures," *Journal of Sound and Vibration*, Vol. 193, No. 5, 1996, pp. 957–983.

[4]Tizzi, S., "Numerical Procedure for the Dynamic Analysis of Three-Dimensional Aeronautical Structures," *Journal of Aircraft*, Vol. 34, No. 1, 1997, pp. 120–130.

[5]Kantorovich, L. V., and Krylov, V. L., *Approximate Methods of Higher Analysis*, Interscience, Inc., New York, 1964, pp. 258–303.

[6]Reddy, J. N., *Applied Functional Analysis and Variational Methods in Engineering*, McGraw–Hill, New York, 1986, pp. 258–285.

[7]Mikhlin, S. G., *Variational Methods in Mathematical Physics*, Pergamon, Oxford, 1964, pp. 74–125.

[8]Fichera, G., *Numerical and Quantitative Analysis*, Pitman, London, Ireland, U.K., 1987, pp. 1–12.

[9]Pars, L. A., *A Treatise of Analytical Dynamics*, Books, Ltd., Belfast, Cambridge, England, U.K., 1968, pp. 34–37.

[10]Kikuchi, N., *Finite Element Method in Mechanics*, Cambridge Univ. Press, 1986, pp. 181–307.

[11]Hughes, T. J. R., *The Finite Element Method, Linear Static and Dynamic Finite Element Analysis*, Prentice–Hall, Upper Saddle River, NJ, 1987, pp. 310–382.

[12]Reddy, J. N., Krishnamoorthy, C. S., and Seetharamu, K. N., *Finite Element Analysis for Engineering Design*, Springer–Verlag, Berlin Heidelberg, 1988, pp. 249–273.

[13]Babuska, I., *The p and h-p Versions of the Finite Element Method. The State of Art. Finite Elements, Theory and Application*, Springer–Verlag, New York, 1988, pp. 199–239.

[14]"The NAG Fortran Library Manual, Mark 17," NAG, Inc., Downers Grove, IL, 1995.

[15]Santini, P., Sneider, M. A., and Leuzzi, L., "Structural Dynamics of Cantilever Swept Wing," *L'Aerotecnica, Missili e Spazio*, Vol. 65, No. 3, 1986, pp. 141–149.

[16]Schaeffer, H. G., *MSC/NASTRAN Primer: Static and Normal Modes, Analysis*, Schaeffer Analysis, Inc., Mount Vernon, NH, 1984, pp. 235–240, 360.

[17]Mindlin, R. D., "Influence of Rotary Inertia and Shear in Flexural Motion of Isotropic, Elastic Plates," *Journal of Applied Mechanics*, Vol. 18, No. 1, 1951, pp. 31–38.

[18]Gould, P. L., *Analysis of Shells and Plates*, Springer–Verlag, New York, 1988, pp. 344–346.

[19]Giles, G. L., "Equivalent Plate Analysis of Aircraft Wing Box Structures with General Planform Geometry," *Journal of Aircraft*, Vol. 23, No. 11, 1986, pp. 859–864.

[20]Giles, G. L., "Further Generalization of an Equivalent Plate Representation for Aircraft Structure Analysis," *Journal of Aircraft*, Vol. 26. No. 1, 1989, pp. 67–74.

[21]Livne, E., "Equivalent Plate Structural Modeling for Wing Shape Optimization Including Transverse Shear," *AIAA Journal*, Vol. 32, No. 6, 1994, pp. 1278–1288.

[22]Livne, E., Sels, R. A., and Bhatia, K. G., "Lessons from Application of Equivalent Plate Structural Modeling to an HSCT Wing," *Journal of Aircraft*, Vol. 31, No. 4, 1994, pp. 953–960.

[23]Livne, E., "Analytical Sensitivities for Shape Optimization in Equivalent Plate Structural Wing Models," *Journal of Aircraft*, Vol. 31, No. 4, 1994, pp. 961–969.